OXFORD

human reproduction

Human Reproduction, 2023, **38(8),** 1538–1546

https://doi.org/10.1093/humrep/dead122

Advance Access Publication Date: June 12, 2023

Original Article

Reproductive biology

Importance of oxygen tension in human ovarian tissue *in vitro* culture

F. Vitale [1], L. Cacciottola[1], F.S. Yu[1], M. Barretta[1], C. Hossay [1], J. Donnez[2,3], and M.M. Dolmans [1,4,*]

[1]Gynecology Research Unit, Institut de Recherche Expérimentale et Clinique, Université Catholique de Louvain, Brussels, Belgium
[2]Société de Recherche pour l'Infertilité, Brussels, Belgium
[3]Université Catholique de Louvain, Brussels, Belgium
[4]Gynecology Department, Cliniques Universitaires Saint-Luc, Brussels, Belgium

*Correspondence address. Gynecology Research Unit, Institut de Recherche Expérimentale et Clinique, Université Catholique de Louvain, Avenue Mounier 52, bte B1.52.02, 1200 Brussels, Belgium. Tel: +32-2-764-5237; Fax: +32-2-764-9507; E-mail: marie-madeleine.dolmans@uclouvain.be https://orcid.org/0000-0002-6331-3026

ABSTRACT

STUDY QUESTION: Is there any difference between 20% and 5% oxygen (O_2) tension *in vitro* culture (IVC) on the viability and quality of human follicles contained in cultured ovarian cortex?

SUMMARY ANSWER: An O_2 tension of 5% yields higher follicle viability and quality than does 20% O_2 tension after 6 days of IVC.

WHAT IS KNOWN ALREADY: The primordial follicle (PMF) pool resides within the ovarian cortex, where the *in vivo* O_2 tension ranges between 2% and 8%. Some studies suggest that lowering O_2 tension to physiological levels may improve *in vitro* follicle quality rates.

STUDY DESIGN, SIZE, DURATION: This prospective experimental study included frozen-thawed ovarian cortex from six adult patients (mean age: 28.5 years; age range: 26–31 years) who were undergoing laparoscopic surgery for non-ovarian diseases. Ovarian cortical fragments were cultured for 6 days at (i) 20% O_2 with 5% CO_2 and (ii) 5% O_2 with 5% CO_2. Non-cultured fragments served as controls.

PARTICIPANTS/MATERIALS, SETTING, METHODS: Cortical fragments were used for the following analyses: hematoxylin and eosin staining for follicle count and classification; Ki67 staining to evaluate PMF proliferation; cleaved caspase-3 immunostaining to identify follicle apoptosis; 8-hydroxy-2-deoxyguanosine and gamma-H2AX (γH2AX) immunolabeling to detect oxidative stress damage and DNA double-strand breaks (DSBs) in oocytes and granulosa cells (GCs); and β-galactosidase staining to assess follicle senescence. Droplet digital PCR was also performed to further explore the gene expression of superoxide dismutase 2 (*SOD2*) and glutathione peroxidase 4 (*GPX4*) from the antioxidant defense system and cyclin-dependent kinase inhibitors (*p21* and *p16*) as tissue senescence-related genes.

MAIN RESULTS AND THE ROLE OF CHANCE: Apoptosis ($P = 0.002$) and follicle senescence ($P < 0.001$) rates were significantly lower in the 5% O_2 group than in the 20% O_2 group. Moreover, GCs in follicles in the 20% O_2 group exhibited significantly ($P < 0.001$) higher oxidative stress damage rates than those in the 5% O_2 group. DNA DSB damage rates in GCs of follicles were also significantly higher ($P = 0.001$) in the 20% O_2 group than in the 5% O_2 group. *SOD2* expression was significantly greater in the 5% O_2 group compared to the 20% O_2 group ($P = 0.04$) and the non-cultured group ($P = 0.002$). Expression of *p21* was significantly increased in both the 20% O_2 ($P = 0.03$) and 5% O_2 ($P = 0.008$) groups compared to the non-cultured group. Moreover, the 20% O_2 group showed significantly greater *p16* expression ($P = 0.04$) than the non-cultured group, while no significant variation was observed between the 5% O_2 and no culture groups.

LARGE SCALE DATA: N/A.

LIMITATIONS, REASONS FOR CAUTION: This study focuses on improving follicle outcomes during the first step of ovarian tissue IVC, where follicles remain *in situ* within the tissue. The impact of O_2 tension in further steps, such as secondary follicle isolation and maturation, was not investigated here.

WIDER IMPLICATIONS OF THE FINDINGS: Our findings suggest that 5% O_2 tension culture is a promising step toward potentially solving the problem of poor follicle viability after IVC.

STUDY FUNDING/COMPETING INTEREST(S): This study was supported by grants from the Fonds National de la Recherche Scientifique de Belgique (FNRS-PDR T.0064.22, CDR J.0063.20 and grant 5/4/150/5 awarded to M.M.D.). The authors have nothing to disclose.

Keywords: fertility preservation / ovarian tissue / in vitro culture / oxygen tension / follicle viability / DNA damage / oxidative stress / cell senescence

Received: February 6, 2023. **Revised:** May 23, 2023. **Editorial decision:** May 30, 2023.

© The Author(s) 2023. Published by Oxford University Press on behalf of European Society of Human Reproduction and Embryology. All rights reserved.
For permissions, please email: journals.permissions@oup.com

Downloaded from https://academic.oup.com/humrep/article/38/8/1538/7194693 by UCLouvain-SCEB user on 08 August 2023

Introduction

Ovarian tissue cryopreservation (OTC) and ovarian tissue transplantation (OTT) have emerged as promising strategies for fertility preservation and endocrine function restoration in patients requiring gonadotoxic therapies (Donnez *et al.*, 2015; Meirow *et al.*, 2016; Donnez and Dolmans, 2017; Dolmans and Manavella, 2019; Yding Andersen *et al.*, 2019). While there is enough evidence to support the feasibility and efficacy of OTC and OTT, there is a risk of reintroducing malignant cells along with the grafted tissue, especially in certain types of cancer, like leukemia, neuroblastoma, and Burkitt's lymphoma (Dolmans *et al.*, 2013b). These patients could potentially benefit from an *in vitro* culture (IVC) system able to support the complete *in vitro* development of early-stage follicles from cryopreserved ovarian tissue into fertilizable oocytes (Telfer *et al.*, 2008). If feasible, ovarian tissue IVC could constitute an alternative to OTT, thereby avoiding the need for a transplantation procedure.

Ideal culture conditions are those that best mimic the *in vivo* physicochemical parameters, including the availability of paracrine factors, nutrients, and oxygen (O_2) (Picton *et al.*, 2008). Indeed, the primordial follicle (PMF) pool resides within the ovarian cortex, where *in vivo* O_2 tension ranges between 2% and 8% (Fischer and Bavister, 1993; Redding *et al.*, 2007, 2008). However, IVC is usually carried out at atmospheric O_2 tension (20%) but still shows unfavorable results. The low follicle survival rates obtained during culture represent the major drawback of this technique, so lowering O_2 tension closer to physiological levels could be considered a strategy to improve follicle outcomes. During the past few years, low O_2 tension IVC has shown encouraging results in animal models. Indeed, culture at 5% O_2 tension was found to significantly increase the viability of cumulus cells (Silva *et al.*, 2009) and follicles in canine ovarian tissue (Pereira *et al.*, 2019) compared to 20% O_2 culture. Moreover, low O_2 tension (5%) promoted oocyte viability and maturation in rat preantral follicle culture (Heise *et al.*, 2009) and enhanced follicle survival in a primate model (Xu *et al.*, 2011). Certainly, supraphysiological O_2 tension (20%) could generate an imbalance between reactive oxygen species (ROS) generation and antioxidant defense mechanisms, resulting in oxidative stress damage (Dröge, 2002). This in turn contributes to mitochondrial dysfunction (Hamanaka and Chandel, 2010) and DNA double-strand breaks (DSBs) (Fang *et al.*, 2014), resulting in cell apoptosis or premature cell senescence (Agarwal *et al.*, 2005; Meuter *et al.*, 2014).

The aim of the present study was to evaluate the effect of 20% and 5% O_2 tension on the viability and quality of human follicles contained within cultured ovarian cortex.

Materials and methods

Experimental design

Frozen-thawed ovarian cortex from six adult patients (mean age: 28.5 years; age range: 26–31 years) undergoing laparoscopic surgery for non-ovarian diseases was fragmented and cultured for 6 days at (i) 20% O_2 with 5% CO_2 or (ii) 5% O_2 with 5% CO_2. After IVC, half of the fragments were embedded in paraffin for further histological, immunolabeling, and gene expression analyses. The other half were frozen in liquid nitrogen-cooled isopentane and stored at −80°C as 10-µm cryosections for subsequent analyses. One fragment per patient served as a non-cultured control.

Ethics approval

Use of human tissue was approved by the Institutional Review Board of the Université Catholique de Louvain, and patients gave their written informed consent for the use of their ovarian tissue for research purposes.

Ovarian tissue cryopreservation and thawing

Ovarian tissue was cryopreserved using a slow-freezing approach at Cliniques Universitaires Saint-Luc, and thawing was done using a fast-thawing procedure, as previously described (Dolmans *et al.*, 2013a).

Biopsy processing and culture technique

After thawing, ovarian biopsies were dissected in 10 ml prewarmed dissection medium to eliminate any surplus medulla, as already reported (Grosbois and Demeestere, 2018; Hossay *et al.*, 2023), and cut into equal fragments of 4 × 2 × 1 mm^3 in size. In total, 24 cortical fragments (two fragments/patient/O_2 group) were individually placed in 4-well culture dishes (Thermo Fisher, Belgium) filled with 300 µl prewarmed culture medium (McCoy's 5a containing bicarbonate supplemented with 25 mM HEPES [Gibco], 0.1% human serum albumin [HSA; CAF-DCF, Belgium], 3 mM glutamine [Sigma], 30 µg/ml penicillin G [Sigma], 50 µg/ml streptomycin [Sigma], 5 µg/ml transferrin [Fisher Scientific], 5 ng/ml selenium [Sigma], 50 µg/ml ascorbic acid [Sigma], 10 ng/ml insulin [Sigma], and 1 ng/ml human follicle-stimulating hormone [FSH; Gonal F, Merck Serono, UK]). Every 2 days, half of the culture medium was replaced.

A low oxygen environment was achieved using a subchamber (ProOx C21, BioSpherix) designed to maintain a controlled gas atmosphere, monitoring the inflow of carbon dioxide (CO_2) and nitrogen (N_2). In the course of continuous sensing, CO_2 and N_2 were infused to reach and sustain O_2 levels at 5%. The subchamber was placed inside an incubator at 37°C, and two wells of sterile distilled water served to maintain culture humidity. To ensure correct levels of O_2 tension in the 5% O_2 group, the culture medium was always pre-equilibrated for 3 h inside the subchamber before use. In addition, the entire medium replacement procedure outside the subchamber never took more than 5 min, not long enough to alter the O_2 tension balance in the medium (Allen *et al.*, 2001).

Sample processing

Cortical fragments were fixed in paraformaldehyde, embedded in paraffin, and cut into 5-µm sections. Hematoxylin and eosin (H&E; Merck, Germany) was used to stain every eighth section to determine follicle count and classification, while those in between underwent immunolabeling and gene expression analysis. All slides were digitized using the Pannoramic P250 Flash III scanner (3DHistech, Hungary) and analyzed by CaseViewer (v2.3).

Histological analysis

Six random H&E-stained sections per sample were examined. To reduce the chances of counting twice, only follicles with a visible oocyte were investigated. Follicles were classified according to the developmental stage into PMFs (including primordial and transitory follicles) and growing follicles (including primary and secondary follicles) (Gougeon and Chainy, 1987), and the percentage of each stage was established. Transitory follicles were included in the PMF group, since these are not entirely distinct entities and share many developmental features with PMFs (Smitz and Cortvrindt, 2002). They are also governed by the same regulatory mechanisms, mainly the phosphatidylinositol-3-kinase (PI3K/AKT), mammalian target of rapamycin (mTOR), and Hippo signaling pathways (Hsueh *et al.*, 2015). Atretic follicles were evaluated according to the following morphological criteria:

Downloaded from https://academic.oup.com/humrep/article/38/8/1538/7194693 by UCLouvain-SCEB user on 08 August 2023

ooplasm eosinophilia, granulosa cell (GC) pyknosis, or cytoplasmic contraction (Gougeon and Chainy, 1987). Vacuolated follicles, including those with vacuoles inside GCs and/or the oocyte, were also calculated as a percentage out of the total number of follicles. PMF and growing follicle density were determined as the number of follicles with normal morphology per mm^3, taking section thickness into account.

Immunohistochemistry

Three non-consecutive sections from each sample were used for immunolabeling for cleaved caspase-3 as a marker of apoptosis and Ki67 to evaluate follicle proliferation. After blocking endogenous peroxidase activity with 3% H_2O_2 and demasking in citrate buffer (pH 6) for 75 min at 98°C, non-specific binding sites were blocked by incubation in 10% fetal bovine serum for 30 min. Sections were first incubated overnight with rabbit monoclonal anti-human caspase-3 primary antibodies (1:200, 9661S; Dako, Glostrup, Denmark) and mouse anti-human Ki67 primary antibodies (1:100, clone MIB1, M7240; Dako). This was followed by incubation with EnVision anti-rabbit horseradish peroxidase (HRP)-conjugated secondary antibodies (1:1, K4003; Dako) for caspase-3 sections and EnVision anti-mouse HRP-conjugated secondary antibodies (1:2, K4001; Dako) for Ki67 sections. Human tonsil and human intestine served as positive controls for caspase-3 and Ki67 staining, and rabbit and mouse immunoglobulin G (Dako) were used for negative controls. For caspase-3 staining, follicles at all stages were evaluated and classified as apoptotic when more than 50% of GCs and/or the oocyte were positive (Amorim et al., 2019). Ki67 analysis was performed only on PMFs, as we were looking to investigate the proliferation rate during their activation from the quiescent state, rather than on growing follicles, which are already known to have undergone proliferation. The following criteria were applied: non-proliferative, when all GCs were negative for Ki67, or proliferative, when at least one GC was positive for Ki67 (Luyckx et al., 2013).

Immunofluorescence

Three non-consecutive sections from each sample were subjected to immunofluorescence for detection of the 8-hydroxy-2-deoxyguanosine (8-OHdG) marker to measure oxidative stress damage and phosphorylated histone H2AX (γH2AX) as a marker of DNA DSBs. After blocking endogenous peroxidase activity with 3% H_2O_2 and demasking in citrate buffer (pH 6) for 75 min at 98°C, non-specific binding sites were blocked by incubation in 10% fetal bovine serum for 30 min. Slides were first incubated with either mouse anti-human 8-OHdG (1:50, MOG-100P; Gentaur, Belgium) or rabbit anti-human γH2AX (1:250, A700-053) primary antibodies, followed by incubation with EnVision mouse HRP (1:1, K001; Dako) for 8-OHdG sections and EnVision rabbit HRP (1:1, K4003; Dako) secondary antibodies for γH2AX sections. They were then incubated for 15 min at room temperature in borate buffer with 30% H_2O_2 (1:1000) and Alexa Fluor 488 tyramide reagent (1:200, B40953; Invitrogen) for γH2AX and 8-OHdG sections as a fluorescent substrate. Cell nuclei were counterstained with Hoechst 33342 (1:1000, H3570, lot 2134015; Invitrogen) and cell membranes were stained with wheat germ agglutinin, CF555 conjugate (1:500, 29076-1; Biotium) diluted in Hank's balanced salt solution (14025-092; Gibco). Human testicular carcinoma was used as a positive control for γH2AX and human skin for 8-OHdG (Supplementary Fig. S1). Mouse and rabbit immunoglobulin G (Dako) were used for negative controls. Follicles showing labeled oocytes or more than 50% of stained GCs were considered positive for both markers. They were expressed as a percentage out of the total number of follicles.

β-Galactosidase activity assays

Half of the fragments were frozen in liquid N_2-cooled isopentane (Cacciottola et al., 2018) and cut into 10-µm cryosections for β-galactosidase (β-gal) activity assays. Toluidine blue was first used to label follicles in cryosections, followed by β-gal staining on directly consecutive sections using the protocol described by Jannone et al. (2020). Human primary sclerosing cholangitis tissue served as positive controls. Two non-consecutive sections from each sample were then selected for analysis of β-gal staining. Slides were digitized with the Pannoramic P250 Flash III slide scanner at 40× magnification. Images of ovarian tissue areas containing follicles were captured with Caseviewer software (v2.2), before computer image analysis using ImageJ software 1.43u (http://rsbweb.nih.gov/ij). Follicles were first digitally isolated from the adjacent stroma with the 'Clear outside' tool option. The 'Color deconvolution, vector: Alcian blue & H' command was then used to convert the RGB image into its different channels (Landini et al., 2021). A threshold was determined to separate β-gal signaling from the rest. After setting the scale of the image, the β-gal-stained area and total area of each follicle were calculated in square micrometers (μm^2) and expressed as a percentage of β-gal staining (Fig. 1).

Gene expression analysis

RNA extraction was performed using the RNeasy FFPE kit (Qiagen, Germany) on 15 formalin-fixed paraffin-embedded tissue sections per sample, according to instructions provided by the manufacturer. Sections were selected based on follicle detection from previous H&E slides, as their distribution is heterogeneous within the ovarian cortex. RNA quality and quantity were assessed using the NanoDrop 2000c spectrophotometer (Thermo Scientific) and Qubit RNA BR assay (Thermo Fisher). RNA samples were reverse-transcribed using SuperScript IV VILO Master Mix (Invitrogen) and cDNA was stored at −80°C. FAM-labeled assays for genes of interest were: *SOD2* (Hs00167309_m1) and *GPX4* (Hs00989766_g1), from the antioxidant defense system, and *p21* (Hs00355782_m1) and *p16* (Hs00923894_m1), as tissue

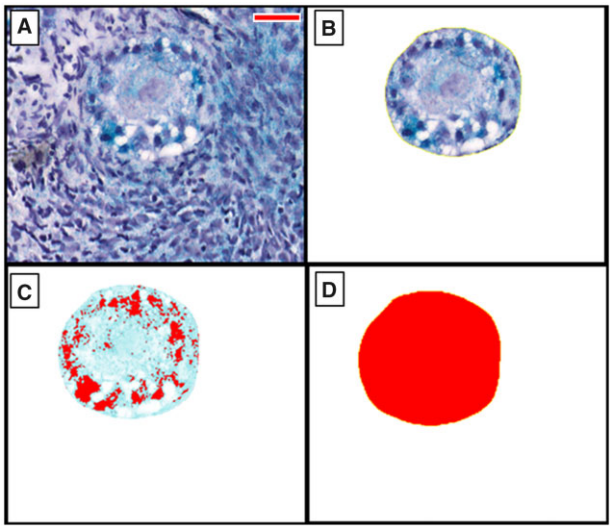


Figure 1. β-gal staining analysis. (**A**) Ovarian follicle surrounded by stromal cells. Scale bar = 20 µm. (**B**) Digital isolation of an ovarian follicle. (**C**) Colour deconvolution and measurement of β-gal area within the follicle. (**D**) Measurement of total follicle area.

Downloaded from https://academic.oup.com/humrep/article/38/8/1538/7194693 by UCLouvain-SCEB user on 08 August 2023

senescence-related genes. Each target assay was duplexed with VIC-labeled assays for the Abelson 1 (ABL-1) (Hs01104728_m1) (Applied Biosystems) reference gene using the QX200 Droplet Digital PCR system (Bio-Rad Laboratories, Hercules, USA).

Statistics

GraphPad Prism software for Windows (v9.2, USA) was used to conduct statistical analyses. Either one-way ANOVA or the Kruskal–Wallis test was applied, followed by Fisher's least significant differences (LSD) or Dunn's multiple comparisons test, depending on the normality of distribution. Data expressed in proportions were analyzed after logit transformation. Results were expressed as mean ± SD. A *P*-value of ≤0.05 was considered statistically significant.

Results

Follicle outcomes

Follicle density and classification

A total of 429 follicles were counted in non-cultured controls, 391 follicles in the 20% O_2 group, and 323 follicles in the 5% O_2 group. There was a significant decrease in PMF density in the 20% O_2 group ($P = 0.03$) compared to the non-cultured group, while no significant variation was observed between the 5% O_2 group and no culture group. When comparing growing follicle density, there was a significant increase in both cultured groups (20% O_2: $P = 0.003$; and 5% O_2: $P = 0.01$) compared to the non-cultured tissue (Fig. 2A). Concerning follicle classification, there was a significant drop in PMF percentages with 20% O_2 (38.67 ± 6.80%, $P < 0.001$) and 5% O_2 (55.17 ± 6.36%, $P < 0.001$) culture compared to the no culture group (80.83 ± 3.65%). However, significantly more PMFs were observed in the 5% O_2 group ($P < 0.001$) than in the 20% O_2 group. In terms of growing follicle proportions, significantly higher rates were observed in the 20% O_2 group (43.17 ± 8.68%, $P < 0.001$) and in the 5% O_2 group (37 ± 7.82%; $P < 0.001$) than in non-cultured tissue (16.50% ± 5.01%) (Fig. 2B). With respect to atresia rates, significantly higher values were encountered in the 20% O_2 group (18.50 ± 3.93%) compared to the 5% O_2 group (7.83 ± 3.06%, $P = 0.01$) and non-cultured tissue (2.50 ± 2.34%, $P < 0.001$) (Fig. 2C and D).

Follicle morphology

Vacuolated follicle percentages were significantly elevated in both the 20% O_2 group (81 ± 11.52%) and the 5% O_2 group (50.17 ± 18.37%) compared to non-cultured tissue (6.83 ± 4.44%, $P < 0.001$). However, the proportion of vacuolated follicles was significantly higher in the 20% O_2 group ($P < 0.001$) than in the 5% O_2 group (Fig. 2E and F).

PMF proliferation

There were 224 PMFs examined in non-cultured controls, 161 in the 20% O_2 group, and 186 in the 5% O_2 group. Percentages of Ki67-positive PMFs were significantly higher in the 20% O_2 group (20.62 ± 8.7%, $P < 0.001$) and in the 5% O_2 group (9.9 ± 6.35%, $P = 0.02$) than in non-cultured fragments (0.7 ± 1.71%), but statistically higher percentages were obtained with 20% O_2 compared to 5% O_2 ($P = 0.01$) (Fig. 2G and H).

Follicle apoptosis

There were 305 follicles analyzed in non-cultured controls and respectively 256 and 253 in the 20% and 5% O_2 groups**.** The percentages of caspase-3-positive follicles were significantly greater in the 20% O_2 group (29.63 ± 10.14%, $P < 0.001$) and in the 5% O_2 group (15.40 ± 4.61%, $P = 0.04$) compared to non-cultured tissue (2.43 ± 3.70%). Nevertheless, significantly higher apoptosis rates were detected with 20% O_2 ($P = 0.002$) than 5% O_2 (Fig. 2I and J) culture.

Oxidative stress response

8 hydroxy-2-deoxyguanosine (8-OHdG) expression

To measure oxidative stress damage, 8-OHdG expression was targeted in oocytes and GCs of follicles (Fig. 3A), as guanosine appears to have the lowest redox potential of all nucleobases (Valavanidis *et al.*, 2009). There were 229 follicles evaluated in non-cultured controls, 210 in the 20% O_2 group, and 174 in the 5% O_2 group. No significant difference was detected in percentages of 8-OHdG-positive oocytes between any of the groups. Regarding GC expression, the 20% O_2 group showed the highest 8-OHdG rate (74.73 ± 15.58%), significantly higher than the 5% O_2 (25.13 ± 4.74%, $P < 0.001$), and no culture (37.60 ± 5.16%, $P < 0.001$) groups. No significant variation was noted between the 5% O_2 group and the non-cultured group (Fig. 3B).

Superoxide dismutase 2 (SOD2) and glutathione peroxidase 4 (GPX4) gene expression

SOD2 and *GPX4* gene expression levels were evaluated to investigate enzymatic scavenger activity between the different groups. The 5% O_2 group yielded significantly higher *SOD2* values (8.28 ± 5.48) than the 20% O_2 group (4.08 ± 1.58, $P = 0.04$) and the non-cultured group (1.36 ± 0.19, $P = 0.002$). *GPX4* gene expression did not exhibit any significant difference between groups (Fig. 3C).

DNA damage rate

γH2AX marker

γH2AX (a specific marker of DNA DSBs) foci were analyzed in oocytes and GCs of follicles (Fig. 3D), including 298 follicles from the non-cultured group, 292 follicles from the 20% O_2 group, and 289 follicles from the 5% O_2 group. No significant variation was found in the percentages of γH2AX-positive oocytes between any of the groups. In GCs, γH2AX-positive follicle rates were significantly higher in the 20% O_2 (34.75 ± 9.92%, $P < 0.001$) and 5% O_2 (19.58 ± 5.43%, $P < 0.001$) compared to the no culture group (0.56 ± 1.38%). However, the rate was significantly ($P = 0.001$) higher in the 20% O_2 group than in the 5% O_2 group (Fig. 3E).

Tissue senescence-related markers

β-gal staining

The β-gal activity assay is a commonly used biomarker of cellular senescence and is elevated due to the accumulation of damaged macromolecules inside lysosomes. Senescent cells are characterized by irreversible cell cycle arrest and secretion of proinflammatory cytokines into the surrounding microenvironment. A total of 274 normal-looking follicles were analyzed for β-gal staining, including 103 from non-cultured controls, and respectively, 91 and 80 follicles from the 20% and 5% O_2 groups. Both 20% O_2 (20.33 ± 7.44%) and 5% O_2 (8 ± 3.08%) groups exhibited significantly greater β-gal staining than non-cultured controls (2.66 ± 1.21%, $P < 0.001$ and $P = 0.04$ respectively), with the 20% O_2 group showing a significantly ($P < 0.001$) higher rate than the 5% O_2 group (Fig. 4A and B).

p21 *and* p16 *gene expression*

Both genes encode cyclin-dependent kinase inhibitors, which function as negative regulators of cell cycle progression. Expression of *p21* was significantly increased in both 20% O_2 (2.36 ± 0.9, $P = 0.03$) and 5% O_2 (2.81 ± 1.19, $P = 0.008$) compared to no culture (0.98 ± 0.95). Moreover, the 20% O_2 group showed significantly greater *p16* expression (0.04 ± 0.05, $P = 0.04$) than the

Downloaded from https://academic.oup.com/humrep/article/38/8/1538/7194693 by UCLouvain-SCEB user on 08 August 2023

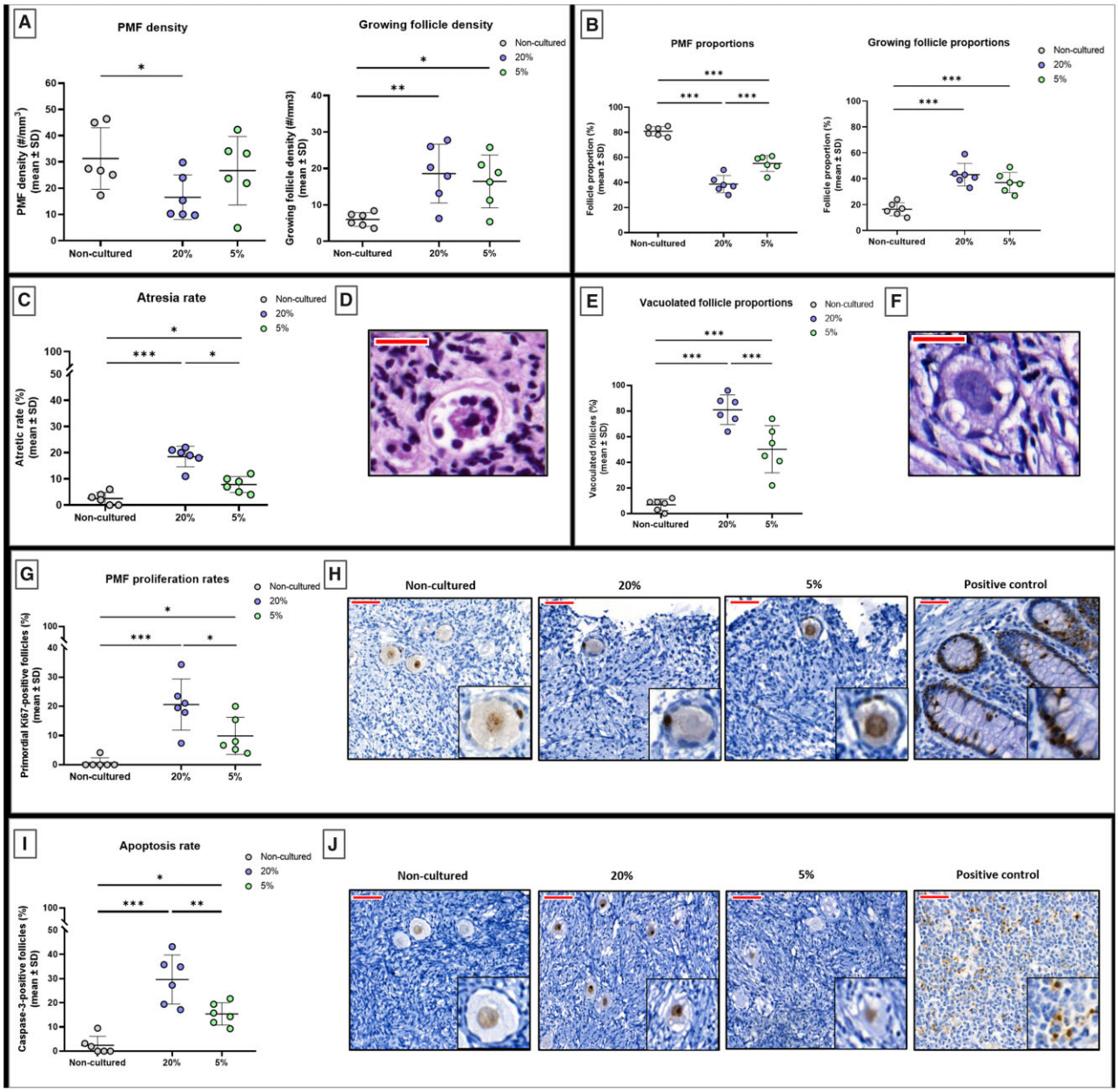


Figure 2. Analyses of follicle density, follicle proportions, atresia, vacuolated follicles, PMF proliferation, and apoptosis. (**A**) Primordial follicle (PMF) and growing follicle density (no. of follicles/mm^3) analyzed by one-way ANOVA and Fisher's least significant differences (LSD) *post hoc* test. (**B**) PMF and growing follicle proportions (percentage, mean ± SD) assessed by one-way ANOVA and Fisher's LSD *post hoc* test. (**C**) Atresia rate (percentage, mean ± SD) determined by one-way ANOVA and Fisher's LSD *post hoc* test. (**D**) Representative photomicrograph of an atretic follicle. Scale bar = 50 µm. (**E**) Vacuolated follicle proportions (percentage, mean ± SD) evaluated by one-way ANOVA and Fisher's least significant differences (LSD) *post hoc* test. (**F**) Representative photomicrograph of a vacuolated follicle. Scale bar = 50 µm. (**G**) PMF proliferation rate (percentage, mean ± SD) calculated by one-way ANOVA and Fisher's LSD *post hoc* test. (**H**) Ki67 immunohistochemical staining in the different groups: non-cultured, 20% O_2, 5% O_2, and positive control (human intestine). Scale bar = 100 µm. (**I**) Apoptosis rate (percentage, mean ± SD) calculated by one-way ANOVA and Fisher's LSD *post hoc* test. (**J**) Cleaved caspase-3 immunohistochemical staining in the different groups: non-cultured, 20% O_2, 5% O_2, and positive control (human tonsil). Scale bar = 100 µm. Significant differences between groups are indicated by *$P < 0.05$; **$P < 0.01$; and ***$P < 0.001$.

non-cultured group (0.01 ± 0.01), while no significant variation was observed between the 5% O_2 and no culture groups (Fig. 4C).

Discussion

For patients at high oncological risk who cannot safely undergo OTT, fertility could potentially be restored by ovarian tissue IVC, growing cryopreserved PMFs into fertile MII oocytes (Telfer and Andersen, 2021). Telfer and colleagues were the first to publish a multistep IVC protocol (McLaughlin *et al.*, 2018), where it was found that the greatest threat to progression occurs during the first step. Indeed, less than a quarter of PMFs within ovarian tissue reach the growth stage (primary or secondary) without any major damage. Among different strategies to optimize preantral follicle development, reducing O_2 tension in IVC has shown the most promising results in animal models. The aim of the present study was to investigate the effects of two different O_2 tension levels (20% and 5%) on human follicles enclosed in the ovarian cortex over the course of 6 days of culture.

Downloaded from https://academic.oup.com/humrep/article/38/8/1538/7194693 by UCLouvain-SCEB user on 08 August 2023

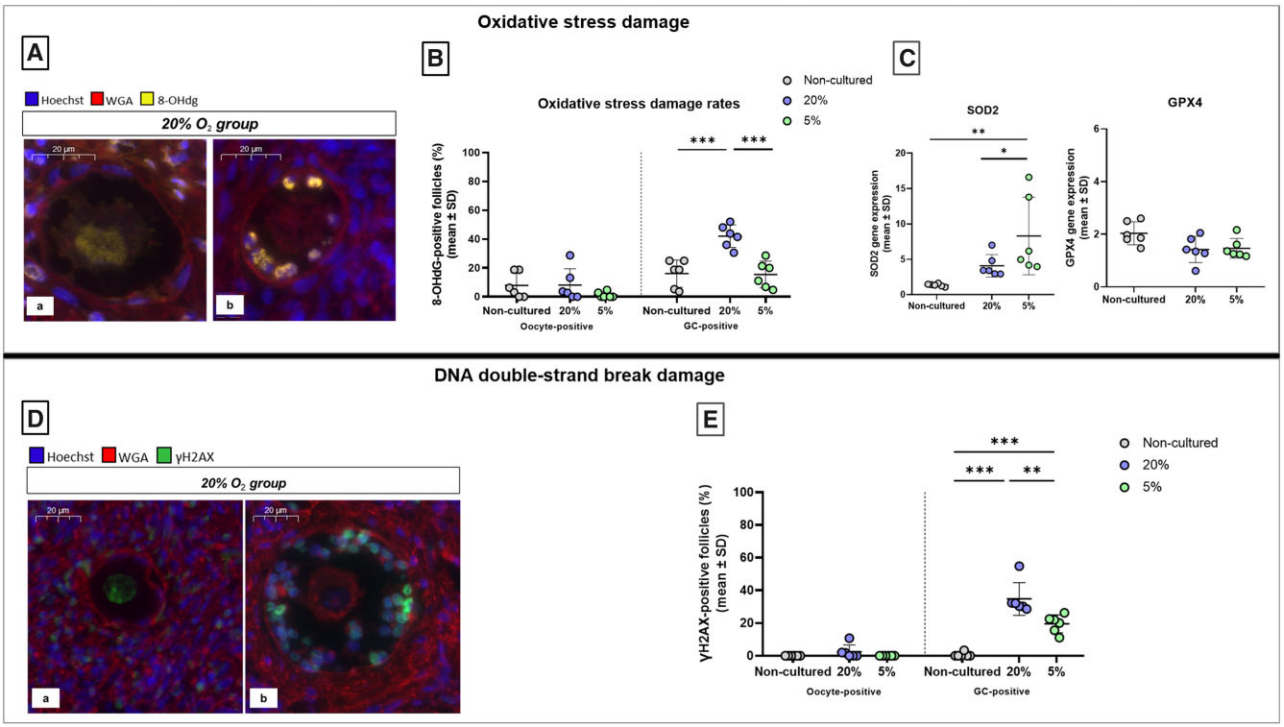


Figure 3. Oxidative stress and DNA double-strand break damage analyses. (**A**) Oxidative stress damage determined by immunofluorescent staining: Hoechst (blue), wheat germ agglutinin (WGA, red), and 8-OHdG (yellow). (**B**) 8-OHdG-positive follicles (percentage, mean ± SD) analyzed by one-way ANOVA and Fisher's least significant differences (LSD) *post hoc* test. (**C**) *SOD2* and *GPX4* gene expression (mean ± SD) determined by one-way ANOVA and Fisher's LSD *post hoc* test. (**D**) DNA DSB damage assessed by immunofluorescent staining for Hoechst (blue), WGA (red), and γH2AX (green). (**E**) γH2AX-positive follicles (percentage, mean ± SD) assessed by one-way ANOVA and Fisher's LSD *post hoc* test. Significant differences between groups are indicated by $^{*}P < 0.05$; $^{**}P < .01$; and $^{***}P < 0.001$.

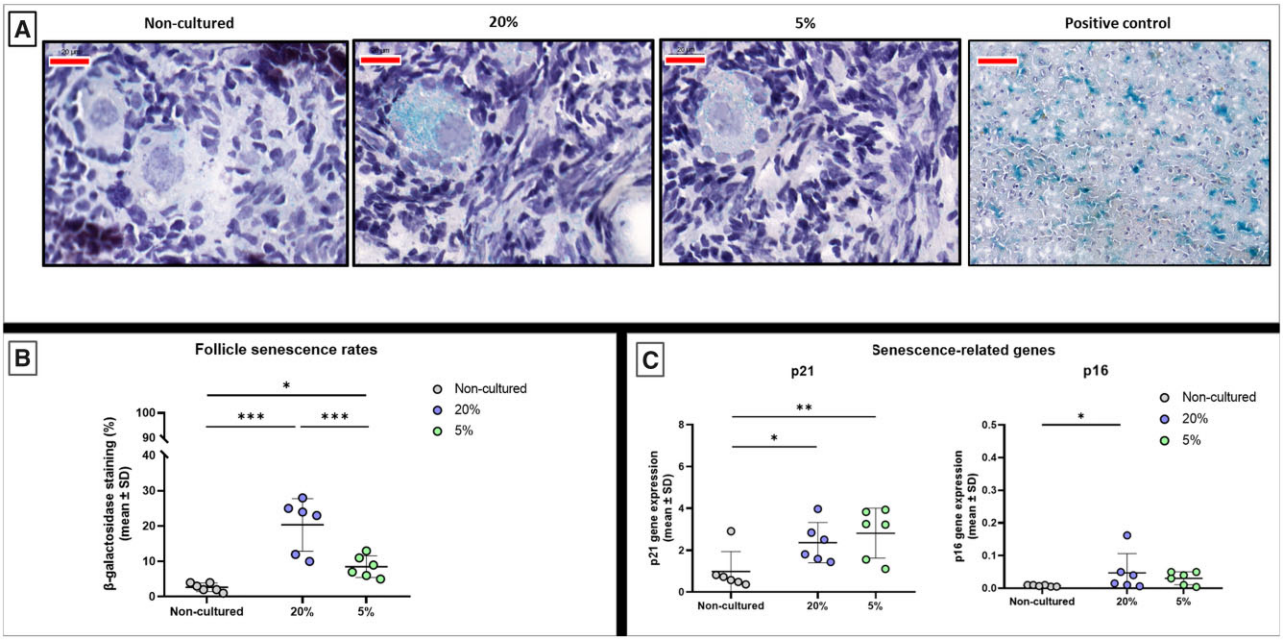


Figure 4. Follicle senescence analyses. (**A**) β-gal staining in the different groups: non-cultured, 20% O_2, 5% O_2, and positive control (human primary sclerosing cholangitis). Scale bar = 20 μm. (**B**) β-gal staining (percentage, mean ± SD) analyzed by one-way ANOVA and Fisher's least significant differences *post hoc* test. (**C**) *p21* and *p16* gene expression (mean ± SD) evaluated by the Kruskal–Wallis test and Dunn's *post hoc* test. Significant differences between groups are indicated by $^{*}P < 0.05$; $^{**}P < 0.01$; and $^{***}P < 0.001$.

Follicle survival rates

It is worth noting that the high intra- and inter-patient heterogeneity of ovarian follicle distribution can lead to considerable variability in follicle density measurements (Schmidt, 2003). This in turn can hamper the ability to reach accurate conclusions based only on this measurement. Moreover, for density analysis, follicles are classified according to their morphology (normal-looking or atretic). However, we believe that this is not the optimal

Downloaded from https://academic.oup.com/humrep/article/38/8/1538/7194693 by UCLouvain-SCEB user on 08 August 2023

way to assess follicle viability, since this classification method does not cover all the molecular mechanisms that precede morphological changes. Follicle apoptosis is a tightly regulated intracellular molecular process that initially involves activation of the caspase family of proteases (Johnson and Bridgham, 2002). Once activated, executive caspases like caspase-3 acquire catalytic functions that lead to morphological changes characteristic of atresia much later (Green and Llambi, 2015). We were able to demonstrate that between the two IVC groups, 5% O_2 yielded the highest follicle survival rates, showed by significantly lower apoptosis rates compared to the 20% O_2 group. These data are in line with previous research in canine cumulus-oocyte complexes, which showed that low O_2 tension (5%) reduces cumulus cell apoptosis more effectively than 20% O_2 (Silva et al., 2009). It has been widely reported that excessive O_2 tension exposure is linked to higher levels of intracellular ROS, which eventually produces oxidative stress damage and promotes cytotoxic activity (Evans et al., 2004; Schieber and Chandel, 2014). To prove the relationship between high O_2 tension exposure and low follicle survival rates, we further investigated the possible mechanisms involved.

Oxidative stress damage

Exposure to supraphysiological O_2 tension levels *in vitro* could ultimately generate disproportionate amounts of oxidants (such as ROS), promoting oxidative stress damage. This may in turn lead to cell apoptosis (Schieber and Chandel, 2014) and result in follicle dysfunction. GCs cultured *in vitro* are reported to be especially sensitive to high ROS exposure (Yang et al., 2017).

Regulation of oxidative stress damage is controlled by enzymatic and non-enzymatic antioxidants, which scavenge ROS accumulation and maintain the redox balance. *SOD2* and *GPX4* gene expression levels were assessed to investigate enzymatic scavenger activity. SOD2, an inducible mitochondrial antioxidant enzyme, catalyzes superoxide anion (O_2^-) into H_2O_2 (Fukai and Ushio-Fukai, 2011), which is then transformed into water and O_2 by the glutathione peroxidase family (GPX1/4) (Kohen and Nyska, 2002). Basini et al. (2004) reported that swine GCs cultured under 5% O_2 tension conditions showed a reduced production of ROS (O_2^- and H_2O_2) and enhanced SOD2 activity. Moreover, addition of exogenous SOD2 resulted in the reduction of cell apoptosis in cultured murine follicles (Tilly and Tilly, 1995). These findings are consistent with the lower rates of oxidative stress and higher levels of *SOD2* expression observed in the current study in the 5% O_2 group compared to the 20% O_2 group.

DNA damage

Among DNA lesions, DSBs are the most deleterious. γH2AX initiates the downstream pathway that triggers DNA damage repair mechanisms in specific DSB sites (Rogakou et al., 1998; Celeste et al., 2003). Nevertheless, persistent DNA DSBs that cannot be properly repaired may ultimately result in genomic instability and cell apoptosis (Zhivotovsky and Kroemer, 2004; Ménézo et al., 2010). Our results showed that 20% O_2 caused greater DNA damage than 5% O_2. High γH2AX expression has been previously associated with concomitantly high oxidative stress damage levels. Meuter and colleagues observed that γH2AX expression levels were elevated in murine blastocysts cultured in 20% O_2 compared to 5% O_2 (Meuter et al., 2014). Moreover, Maidarti et al. (2020) demonstrated the association between increased follicle proliferation rates and impaired follicle health, with an increase in DNA damage markers (γH2AX).

Although at first glance it might appear favorable, accelerated *in vitro* proliferation has been linked to a decline in follicle quality as they undergo further development (McLaughlin et al., 2014) and to ovarian pathology in a murine model (Kim et al., 2015). This uncontrolled proliferation is markedly different from the physiological circumstances in which PMFs undergo a gradual process of activation prior to entering the different stages of development. The current study demonstrates that higher rates of DNA damage are associated with greater PMF proliferation in tissue cultured at 20% O_2 compared to 5% O_2 tension. While IVC techniques increasing the proliferation of PMFs may seem promising, the associated impairment of follicle health and quality should not be overlooked. Taken together, these findings suggest that culture under physiological oxygen conditions improves the coordination of early development and the quality of the follicles cultured *in vitro*.

Senescence-related response

Cellular senescence is characterized by stable cell cycle arrest induced by multiple stress stimuli, such as telomere shortening, oxidative stress, and DNA damage (Parrinello et al., 2003; Fumagalli et al., 2012). Senescence is activated as a response to cell impairment, enabling the suppression of potentially dysfunctional cells (Kuilman et al., 2010). In our study, the 20% O_2 group showed significantly greater follicle β-gal staining rates than the 5% O_2 group, strongly indicating that supraphysiological O_2 tension levels are perceived as stressful by human ovarian follicles *in vitro*. The same results appear to show that oxidative stress damage, DNA DSBs, and replicative senescence may be associated, as they were all elevated at 20% O_2 compared to 5% O_2. In line with the current data, Seno and colleagues demonstrated that culturing human trophoblast cells at 20% O_2 significantly increased cell senescence rates compared to 5% O_2 tension (Seno et al., 2018). Moreover, excessive ROS accumulation has been reported to be a powerful *in vitro* human GC senescence inducer and has been linked to decreased oocyte developmental competence (Lin et al., 2020).

Furthermore, we studied the expression of *p21* and *p16* genes, which are cyclin-dependent kinase inhibitors involved in cell cycle arrest (Hernandez-Segura et al., 2018). Cellular senescence has two differentiated stages: (i) early-stage senescence characterized by upregulation of p21, which suppresses cyclin E; and (ii) late-stage senescence with activation of p16, which inhibits cyclin D1 expression (Stein et al., 1999). In the current study, the 20% O_2 group showed increased expression of both *p21* and *p16* compared to non-cultured tissue, while the 5% O_2 group only exhibited an increase in *p21*. These findings strongly suggest that culture at 20% O_2 tension could initiate earlier onset of follicle senescence than culture at 5% O_2, since both markers were upregulated in the former group. It is well known that the accumulation of ROS-induced oxidative stress damage within cells is a key factor in triggering senescence (Chistiakov et al., 2014). ROS damage to mitochondrial components eventually provokes cytotoxicity and enters a feedback loop, producing yet more ROS as a result (De Gaetano et al., 2021). Hence, high oxidative stress levels often create a vicious cycle during senescence. As far as we know, this is the first study to describe the negative impact of high O_2 tension on human ovarian follicle IVC in terms of the senescence pathway.

Conclusion

This study provides compelling evidence that O_2 tension is a crucial factor influencing the health of human ovarian follicles during *in vitro* culture. Culture at 5% O_2 tension creates an

Downloaded from https://academic.oup.com/humrep/article/38/8/1538/7194693 by UCLouvain-SCEB user on 08 August 2023

environment that more accurately mimics the physiological conditions *in vivo*, resulting in the improved coordination of follicle proliferation and initial development *in vitro*. This beneficial effect is attributed to the lower levels of oxidative stress-related lesions and DNA DSBs observed at 5% compared to 20% O_2 tension. Further research is needed to establish optimal culture conditions for ovarian tissue IVC systems before this technique can be contemplated in clinical practice.

Supplementary data

Supplementary data are available at *Human Reproduction* online.

Data availability

Data underlying this article will be shared upon reasonable request addressed to the corresponding author.

Acknowledgements

The authors thank Mira Hryniuk, BA, for reviewing the English language of the article and Dolores Gonzalez, Olivier Van Kerk, and Sarah Storder for their technical assistance.

Authors' roles

F.V.: Experimental design, experimental procedures, analyses, statistical analysis, interpretation of results, and article preparation. L.C.: Experimental design, statistical analysis, and interpretation of results. F.S.Y.: Experimental procedures and analyses. M.B.: Experimental procedures and analyses. C.H.: Experimental procedures. J.D.: Interpretation of results, article preparation and revision. M.M.D.: Experimental design, interpretation of results, article preparation, and revision.

Funding

The Fonds National de la Recherche Scientifique de Belgique (FNRS-PDR T.0064.22, CDR J.0063.20 and grant 5/4/150/5 awarded to M.M.D.).

Conflict of interest

The authors have nothing to disclose.

References

Agarwal A, Gupta S, Sharma RK. Role of oxidative stress in female reproduction. *Reprod Biol Endocrinol* 2005;**3**:28.

Allen CB, Schneider BK, White CW. Limitations to oxygen diffusion and equilibration in in vitro cell exposure systems in hyperoxia and hypoxia. *Am J Physiol Lung Cell Mol Physiol* 2001;**281**: L1021–1027.

Amorim CA, Donnez J, Dehoux J-P, Scalercio SR, Squifflet J, Dolmans M-M. Long-term follow-up of vitrified and autografted baboon (*Papio anubis*) ovarian tissue. *Hum Reprod* 2019;**34**:323–334.

Basini G, Grasselli F, Bianco F, Tirelli M, Tamanini C. Effect of reduced oxygen tension on reactive oxygen species production and activity of antioxidant enzymes in swine granulosa cells. *Biofactors* 2004;**20**:61–69.

Cacciottola L, Manavella DD, Amorim CA, Donnez J, Dolmans M-M. In vivo characterization of metabolic activity and oxidative stress in grafted human ovarian tissue using microdialysis. *Fertil Steril* 2018;**110**:534–544.e3.

Celeste A, Fernandez-Capetillo O, Kruhlak MJ, Pilch DR, Staudt DW, Lee A, Bonner RF, Bonner WM, Nussenzweig A. Histone H2AX phosphorylation is dispensable for the initial recognition of DNA breaks. *Nat Cell Biol* 2003;**5**:675–679.

Chistiakov DA, Sobenin IA, Revin VV, Orekhov AN, Bobryshev YV. Mitochondrial aging and age-related dysfunction of mitochondria. *BioMed Res Int* 2014;**2014**:1–7.

De Gaetano A, Gibellini L, Zanini G, Nasi M, Cossarizza A, Pinti M. Mitophagy and oxidative stress: the role of aging. *Antioxidants* 2021;**10**:794.

Dolmans M-M, Jadoul P, Gilliaux S, Amorim CA, Luyckx V, Squifflet J, Donnez J, Van Langendonckt A. A review of 15 years of ovarian tissue bank activities. *J Assist Reprod Genet* 2013a;**30**:305–314.

Dolmans M-M, Luyckx V, Donnez J, Andersen CY, Greve T. Risk of transferring malignant cells with transplanted frozen-thawed ovarian tissue. *Fertil Steril* 2013b;**99**:1514–1522.

Dolmans M-M, Manavella DD. Recent advances in fertility preservation: advances in fertility preservation. *J Obstet Gynaecol Res* 2019; **45**:266–279.

Donnez J, Dolmans M-M. Fertility preservation in women. *N Engl J Med* 2017;**377**:1657–1665.

Donnez J, Dolmans M-M, Diaz C, Pellicer A. Ovarian cortex transplantation: time to move on from experimental studies to open clinical application. *Fertil Steril* 2015;**104**:1097–1098.

Dröge W. Free radicals in the physiological control of cell function. *Physiol Rev* 2002;**82**:47–95.

Evans MD, Dizdaroglu M, Cooke MS. Oxidative DNA damage and disease: induction, repair and significance. *Mutat Res* 2004;**567**:1–61.

Fang X, Ide N, Higashi S-I, Kamei Y, Toyooka T, Ibuki Y, Kawai K, Kasai H, Okamoto K, Arimoto-Kobayashi S *et al.* Somatic cell mutations caused by 365 nm LED-UVA due to DNA double-strand breaks through oxidative damage. *Photochem Photobiol Sci* 2014;**13**:1338–1346.

Fischer B, Bavister BD. Oxygen tension in the oviduct and uterus of rhesus monkeys, hamsters and rabbits. *J Reprod Fertil* 1993;**99**: 673–679.

Fukai T, Ushio-Fukai M. Superoxide dismutases: role in redox signaling, vascular function, and diseases. *Antioxid Redox Signal* 2011; **15**:1583–1606.

Fumagalli M, Rossiello F, Clerici M, Barozzi S, Cittaro D, Kaplunov JM, Bucci G, Dobreva M, Matti V, Beausejour CM *et al.* Telomeric DNA damage is irreparable and causes persistent DNA-damage-response activation. *Nat Cell Biol* 2012;**14**:355–365.

Gougeon A, Chainy GBN. Morphometric studies of small follicles in ovaries of women at different ages. *J Reprod Fertil* 1987;**81**: 433–442.

Green DR, Llambi F. Cell death signaling. *Cold Spring Harb Perspect Biol* 2015;**7**:a006080.

Grosbois J, Demeestere I. Dynamics of PI3K and Hippo signaling pathways during in vitro human follicle activation. *Hum Reprod* 2018;**33**:1705–1714.

Hamanaka RB, Chandel NS. Mitochondrial reactive oxygen species regulate cellular signaling and dictate biological outcomes. *Trends Biochem Sci* 2010;**35**:505–513.

Heise MK, Koepsel R, McGee EA, Russell AJ. Dynamic oxygen enhances oocyte maturation in long-term follicle culture. *Tissue Eng C: Methods* 2009;**15**:323–332.

Hernandez-Segura A, Nehme J, Demaria M. Hallmarks of cellular senescence. *Trends Cell Biol* 2018;**28**:436–453.

Hossay C, Tramacere F, Cacciottola L, Camboni A, Squifflet J-L, Donnez J, Dolmans M-M. Follicle outcomes in human ovarian

Downloaded from https://academic.oup.com/humrep/article/38/8/1538/7194693 by UCLouvain-SCEB user on 08 August 2023

tissue: effect of freezing, culture, and grafting. *Fertil Steril* 2023; **119**:135–145.

Hsueh AJW, Kawamura K, Cheng Y, Fauser BCJM. Intraovarian control of early folliculogenesis. *Endocr Rev* 2015;**36**:1–24.

Jannone G, Rozzi M, Najimi M, Decottignies A, Sokal EM. An optimized protocol for histochemical detection of senescence-associated beta-galactosidase activity in cryopreserved liver tissue. *J Histochem Cytochem* 2020;**68**:269–278.

Johnson AL, Bridgham JT. Caspase-mediated apoptosis in the vertebrate ovary. *Reproduction* 2002;**124**:19–27.

Kim S-Y, Ebbert K, Cordeiro MH, Romero M, Zhu J, Serna VA, Whelan KA, Woodruff TK, Kurita T. Cell autonomous phosphoinositide 3-kinase activation in oocytes disrupts normal ovarian function through promoting survival and overgrowth of ovarian follicles. *Endocrinology* 2015;**156**:1464–1476.

Kohen R, Nyska A. Oxidation of biological systems: oxidative stress phenomena, antioxidants, redox reactions, and methods for their quantification. *Toxicol Pathol* 2002;**30**:620–650.

Kuilman T, Michaloglou C, Mooi WJ, Peeper DS. The essence of senescence: figure 1. *Genes Dev* 2010;**24**:2463–2479.

Landini G, Martinelli G, Piccinini F. Colour deconvolution: stain unmixing in histological imaging. *Bioinformatics* 2021;**37**: 1485–1487.

Lin X, Dai Y, Tong X, Xu W, Huang Q, Jin X, Li C, Zhou F, Zhou H, Lin X *et al.* Excessive oxidative stress in cumulus granulosa cells induced cell senescence contributes to endometriosis-associated infertility. *Redox Biol* 2020;**30**:101431.

Luyckx V, Scalercio S, Jadoul P, Amorim CA, Soares M, Donnez J, Dolmans M-M. Evaluation of cryopreserved ovarian tissue from prepubertal patients after long-term xenografting and exogenous stimulation. *Fertil Steril* 2013;**100**:1350–1357.

Maidarti M, Anderson RA, Telfer EE. Crosstalk between PTEN/PI3K/Akt signalling and DNA damage in the oocyte: implications for primordial follicle activation, oocyte quality and ageing. *Cells* 2020;**9**:200.

McLaughlin M, Albertini DF, Wallace WHB, Anderson RA, Telfer EE. Metaphase II oocytes from human unilaminar follicles grown in a multi-step culture system. *Mol Hum Reprod* 2018;**24**:135–142.

McLaughlin M, Kinnell HL, Anderson RA, Telfer EE. Inhibition of phosphatase and tensin homologue (PTEN) in human ovary in vitro results in increased activation of primordial follicles but compromises development of growing follicles. *Mol Hum Reprod* 2014;**20**:736–744.

Meirow D, Ra'anani H, Shapira M, Brenghausen M, Derech Chaim S, Aviel-Ronen S, Amariglio N, Schiff E, Orvieto R, Dor J. Transplantations of frozen-thawed ovarian tissue demonstrate high reproductive performance and the need to revise restrictive criteria. *Fertil Steril* 2016;**106**:467–474.

Ménézo Y, Dale B, Cohen M. DNA damage and repair in human oocytes and embryos: a review. *Zygote* 2010;**18**:357–365.

Meuter A, Rogmann L-M, Winterhoff BJ, Tchkonia T, Kirkland JL, Morbeck DE. Markers of cellular senescence are elevated in murine blastocysts cultured in vitro: molecular consequences of culture in atmospheric oxygen. *J Assist Reprod Genet* 2014;**31**: 1259–1267.

Parrinello S, Samper E, Krtolica A, Goldstein J, Melov S, Campisi J. Oxygen sensitivity severely limits the replicative lifespan of murine fibroblasts. *Nat Cell Biol* 2003;**5**:741–747.

Pereira LMC, Lopes MD, Songsasen N. Effect of oxygen tension on in vitro viability and development of dog follicles enclosed within the ovarian cortex. *Reprod Domest Anim* 2019;**54**:1139–1144.

Picton HM, Harris SE, Muruvi W, Chambers EL. The in vitro growth and maturation of follicles. *Reproduction* 2008;**136**:703–715.

Redding GP, Bronlund JE, Hart AL. Mathematical modelling of oxygen transport-limited follicle growth. *Reproduction* 2007;**133**: 1095–1106.

Redding GP, Bronlund JE, Hart AL. Theoretical investigation into the dissolved oxygen levels in follicular fluid of the developing human follicle using mathematical modelling. *Reprod Fertil Dev* 2008;**20**:408–417.

Rogakou EP, Pilch DR, Orr AH, Ivanova VS, Bonner WM. DNA double-stranded breaks induce histone H2AX phosphorylation on serine 139. *J Biol Chem* 1998;**273**:5858–5868.

Schieber M, Chandel NS. ROS function in redox signaling and oxidative stress. *Curr Biol* 2014;**24**:R453–R462.

Schmidt KLT, Byskov AG, Nyboe Andersen A, Müller J, Yding Andersen C. Density and distribution of primordial follicles in single pieces of cortex from 21 patients and in individual pieces of cortex from three entire human ovaries. *Hum Reprod* 2003;**18**: 1158–1164.

Seno K, Tanikawa N, Takahashi H, Ohkuchi A, Suzuki H, Matsubara S, Iwata H, Kuwayama T, Shirasuna K. Oxygen concentration modulates cellular senescence and autophagy in human trophoblast cells. *Am J Reprod Immunol* 2018;**79**:e12826.

Silva A, Rodriguez P, Cavalcante L, Rodrigues B, Rodrigues J. The influence of oxygen tension on cumulus cell viability of canine COCs matured in high-glucose medium. *Reprod Domest Anim* 2009;**44**:259–262.

Smitz J, Cortvrindt R. The earliest stages of folliculogenesis in vitro. *Reproduction* 2002;**123**:185–202.

Stein GH, Drullinger LF, Soulard A, Dulić V. Differential roles for cyclin-dependent kinase inhibitors p21 and p16 in the mechanisms of senescence and differentiation in human fibroblasts. *Mol Cell Biol* 1999;**19**:2109–2117.

Telfer EE, Andersen CY. In vitro growth and maturation of primordial follicles and immature oocytes. *Fertil Steril* 2021;**115**: 1116–1125.

Telfer EE, McLaughlin M, Ding C, Thong KJ. A two-step serum-free culture system supports development of human oocytes from primordial follicles in the presence of activin. *Hum Reprod* 2008; **23**:1151–1158.

Tilly JL, Tilly KI. Inhibitors of oxidative stress mimic the ability of follicle-stimulating hormone to suppress apoptosis in cultured rat ovarian follicles. *Endocrinology* 1995;**136**:242–252.

Valavanidis A, Vlachogianni T, Fiotakis C. 8-hydroxy-2'-deoxyguanosine (8-OHdG): a critical biomarker of oxidative stress and carcinogenesis. *J Environ Sci Health C: Environ Carcinog Ecotoxicol Rev* 2009;**27**:120–139.

Xu J, Lawson MS, Yeoman RR, Pau KY, Barrett SL, Zelinski MB, Stouffer RL. Secondary follicle growth and oocyte maturation during encapsulated three-dimensional culture in rhesus monkeys: effects of gonadotrophins, oxygen and fetuin. *Hum Reprod* 2011;**26**:1061–1072.

Yang H, Xie Y, Yang D, Ren D. Oxidative stress-induced apoptosis in granulosa cells involves JNK, p53 and Puma. *Oncotarget* 2017;**8**: 25310–25322.

Yding Andersen C, Mamsen LS, Kristensen SG. FERTILITY PRESERVATION: freezing of ovarian tissue and clinical opportunities. *Reproduction* 2019;**158**:F27–F34.

Zhivotovsky B, Kroemer G. Apoptosis and genomic instability. *Nat Rev Mol Cell Biol* 2004;**5**:752–762.

Downloaded from https://academic.oup.com/humrep/article/38/8/1538/7194693 by UCLouvain-SCEB user on 08 August 2023